
Friedl J, Lebedeva MA, Porfyrakis K, Stimming U, Chamberlain TW. [All fullerene-based cells for non-aqueous redox flow batteries](#). *Journal of the American Chemical Society* 2017

Copyright:

This document is the Accepted Manuscript version of a Published Work that appeared in final form in *Journal of the American Chemical Society*, copyright © American Chemical Society after peer review and technical editing by the publisher. To access the final edited and published work see:

DOI link to article:

<https://doi.org/10.1021/jacs.7b11041>

Date deposited:

19/12/2017

Embargo release date:

12 December 2018



This work is licensed under a [Creative Commons Attribution-NonCommercial 3.0 Unported License](#)

All fullerene-based cells for non-aqueous redox flow batteries

Jochen Friedl,[†] Maria. A. Lebedeva,[‡] Kyriakos Porfyrakis,[‡] Ulrich Stimming^{*,†} and Thomas W. Chamberlain^{*,§}

[†]School of Natural and Environmental Sciences, Newcastle University, Newcastle upon Tyne, NE1 7RU, UK

[‡]Department of Materials, University of Oxford, 16 Parks Road, Oxford, OX1 3PH, UK

[§]Institute of Process Research and Development, School of Chemistry, University of Leeds, Leeds, LS2 9JT, UK

Supporting Information Placeholder

ABSTRACT: Redox flow batteries have the potential to revolutionize our use of intermittent sustainable energy sources such as solar and wind power by storing the energy in liquid electrolytes. Our concept study utilizes a novel electrolyte system, exploiting derivatised fullerenes as both anolyte and catholyte species in a series of battery cells, including a symmetric, single species system which alleviates the common problem of membrane crossover. The prototype multi electron system, utilizing molecular based charge carriers, made from inexpensive, abundant and sustainable materials, principally, C and Fe, demonstrates remarkable current and energy densities and promising long-term cycling stability.

Redox flow batteries (RFBs) represent an exciting opportunity to tackle the problem of energy storage, offering the potential of large scale, affordable and safe systems. Generally external energy is utilised to drive the cell reaction in a thermodynamically uphill direction, by generating oxidised species at the cathode and reduced species at the anode, after which the species are flowed into a tank and stored until the energy is required. To release the stored energy the system is discharged by flowing species back into the cell to react at the electrodes. The efficiency of this process depends on several factors including; the concentration of reactive species in the solutions, the formal potential of the redox couples, the kinetics of the electrochemical processes, and the stability of the active species. As well as this, it is important to consider the safety and cost of the active materials if scale-up is going to be viable.¹ A number of candidate materials have been proposed and explored as redox species in recent years including aqueous systems with all-vanadium (VRB), iron-chromium, polysulfide-bromine redox couples.² Such systems, though effective, generally suffer from low power- and energy-density, and in the case of the all-vanadium system, high overall costs due to the expensive active species.

Recently, a number of novel chemistries have been proposed that utilize organic redox electrolytes prepared from inexpensive precursors. For example, in aqueous solvents hydroxylated anthraquinones (AQDS),^{3,4} hexacyanoferrate,⁴ viologen and ferrocene⁵ and redox-active polymers⁶ were reported. Non-aqueous chemistries employing phenothiazine derivatives,⁷ benzothiadiazole,⁸ 2,5-di-tert-butyl-1-methoxy-4-[2-methoxyethoxy]benzene as catholyte with 9-fluorenone⁹ or N-methylphthalimide¹⁰ (NMP) as anolyte have been reported with high solubility (> 0.3 M) of the redox species. For recent reviews on chemistries for RFBs please see^{11–13}. While these systems propose avenues to reach the Advanced Projects Research Agency-Energy (ARPA-e) defined goal of \$100 kW h^{-1} , none of the reported systems are able to emulate the biggest advantage of the VRB: Usage of an electrolyte with a single redox

active molecule which remedies irreversible capacity loss due to cross-over through the membrane.

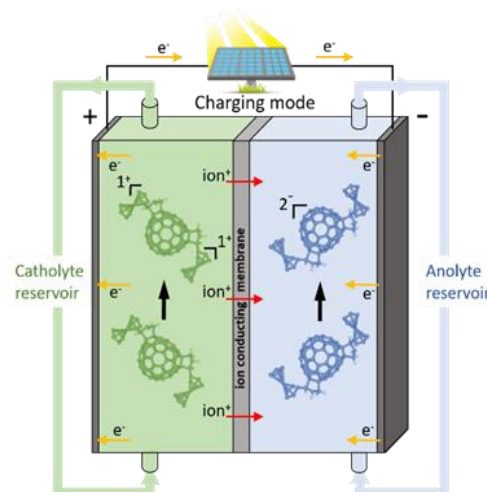
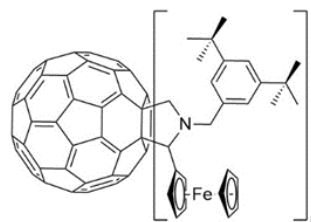


Figure 1. Schematic of the all fullerene RFB setup.



Scheme 1. Functionalised fullerene derivatives 1-4 ($n=1-4$).

Fullerene derivatives have the capacity to accept multiple electrons, undergo very fast and stable fullerene cage based redox processes,¹⁴ are reasonably cheap and abundant, as a result of C₆₀ being the thermodynamically most stable form of molecular carbon, and can be made extremely soluble in organic¹⁵ and aqueous¹⁶ solvents with appropriate modification. It is therefore remarkable that they have never been explored as candidates for the redox species in RFBs previously. Fullerene derivatives decorated with suitable electron donating groups can form a species with at least three oxidation states which are separated by more than 1 V, so that one molecule can serve both as anolyte and catholyte and cross-over does not chemically contaminate the electrolytes (see Fig. 1a).

Herein, we explore the unique concept of an all fullerene based cell, employing an appropriately derivatised fullerene as active species in both catholyte and anolyte as schematically demonstrated in Figure 1. We utilise multiple metallocene moieties appended to the

fullerene cage as the catholyte species, while exploiting the inherent, reversible redox processes of the fullerene moiety as the anode-active species. A series of functionalised fullerenes were synthesised containing a number of appended ferrocene units ranging from 1 to 4, **1-4**, Scheme 1 (see ESI file for full experimental details).

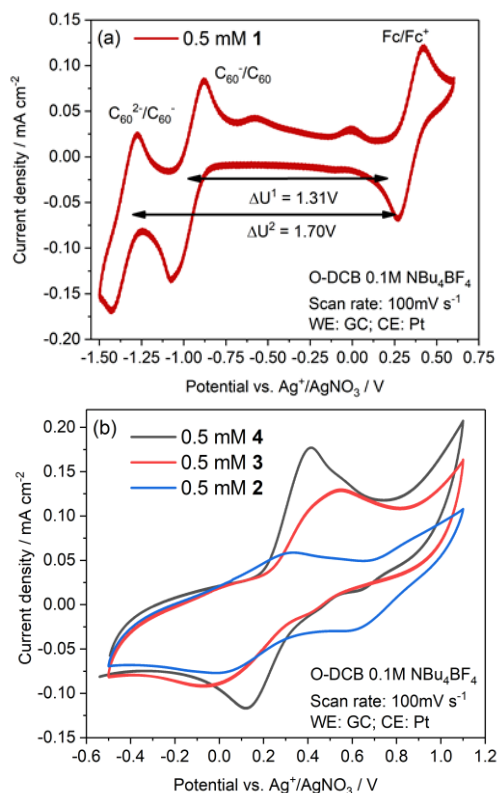


Figure 2. Cyclic voltammograms of (a) **1** and (b) **2**, **3**, and **4** in *O*-DCB with 0.1 M NBu₄BF₄ as supporting electrolyte.

The fullerene derivatives were observed to be soluble in a variety of solvents and exhibited remarkably high solubility in ortho-dichlorobenzene (*O*-DCB) (c.f. solubility of **4** in *O*-DCB = 300 ± 22 mg/mL) with a general trend of higher solubility upon addition of more ferrocene moieties (see ESI file). The redox properties of **1-4** were investigated using cyclic voltammetry in *O*-DCB with NBu₄BF₄ as the supporting electrolyte. All potentials are reported versus Ag⁺/AgNO₃. Figure 2a shows two consecutive 1-electron waves associated with reduction and oxidation of the C₆₀-cage of **1** at low potentials, $U_0^{C_{60},1} = -0.97$ V and $U_0^{C_{60},2} = -1.36$ V, and the redox wave for the attached ferrocene at $U_0^{Fc} = 0.34$ V. This indicates that a single molecule, **1**, transfers two electrons at a potential suitable for an anolyte, and one electron at significantly higher potential. In a battery, potential differences of $\Delta U^1 = 1.31$ V and $\Delta U^2 = 1.70$ V could therefore be established. Employing sampled current voltammetry (SCV) we determined a rate constant for the Fc/Fc⁺ redox reaction of at least $k_0^{1,Fc} = 0.397$ cm s⁻¹ and a transfer coefficient of $\alpha = 0.60$ (see Fig. S7). This is similar to values of $k_0^{Fc} = 1.02 \pm 0.009$ cm s⁻¹ and $\alpha = 0.60 \pm 0.05$ determined for freely diffusing ferrocene/ferrocenium in acetonitrile by SCV on microelectrodes.¹⁷ The kinetics observed are orders of magnitudes higher than for other redox couples employed in RFBs (e.g. VO²⁺/VO₂⁺: $k_0 = 10^{-6}$ cm s⁻¹).¹⁸

The standard potentials of the C₆₀ reductions are given in Table S2 and shown in Fig. S6. As expected, due to the saturation of double bonds on the molecule, the potentials for the C₆₀ reductions shift

to more negative values for higher Fc adducts.¹⁹ Good cycling stability was demonstrated for **4**, which showed no change in its electrochemical response when cycled 100 times (see Fig. S7). Initial battery studies were performed in a stationary cell optimised for small volumes of electrolyte. Two carbon felt electrodes were soaked in anolyte and catholyte solution respectively and separated by a glass fiber separator. Absorption experiments established that the absorption of fullerene-ferrocene derivatives on the carbon felt is negligible (see Table S6). Preliminary tests were performed to confirm that capacitive processes do not contribute to the measured capacity of fullerene-based cells (Fig. S10). A cell with 4 mM ferrocene as catholyte and 2 mM indene-C₆₀ bis-adduct (ICBA), a commercially available fullerene, as anolyte showed a negligible discharge capacity (Fig. S10), indicating that free Fc is not a suitable catholyte, despite its application as redox-shuttle in mediated RFBs.²⁰ This might be due to cross-over of the comparatively small Fc molecule through the separator. The fullerene cage of the molecule in the anolyte, ICBA, exhibited redox waves like the C₆₀/C₆₀⁻ and C₆₀⁻/C₆₀²⁻ waves of **1** (compare Fig. S9 and Fig 2a).

Four cells were constructed using *O*-DCB and 0.1 M NBu₄BF₄ to test different fullerene-based cell chemistries. Fig. 3a shows a cell utilising the Fc/Fc⁺ redox reactions of **2** as catholyte and the C₆₀ redox reactions of ICBA, as anolyte. This is referred to as the **2**/ICBA cell, and with 1 mM of 2 electron transferring molecules **2** and ICBA, has a theoretical capacity, Q^{theo} , of 0.038 mA h. This value is almost reached in discharge cycles 1-5 at a current of 0.5 mA. The difference in charging voltage to discharge voltage is high, implying a low voltage efficiency for the **2**/ICBA cell in *O*-DCB. However, the average voltage locations match with the potential positions for the redox reactions shown in Fig. 2a, indicating that Plateau I stems from the peaks constituting $\Delta U^1 = 1.31$ V, and Plateau II from those that make up $\Delta U^2 = 1.70$ V. The simple glass fibre separator prevents instantaneous cross-over and is therefore an easy and inexpensive solution, working solely on size exclusion which is especially suitable for symmetric systems like **2**/**2**. 100 cycles of charge and discharge were investigated for 1 mM solutions of the more highly derivatised fullerene molecules **3** and **4** versus an appropriate concentration of ICBA to balance the charge of the functionalised C₆₀. These cells are labelled **3**/ICBA (Fig. S11) and **4**/ICBA respectively, with the curves for the latter shown in Fig. 3b. One more cell, **2**/**2**, with **2** as both as anolyte and catholyte showcases the concept of a symmetric RFB chemistry with fullerene derivatives (Fig S12). This symmetric chemistry has the advantage that any cross-over of redox species through the separator does not lead to a chemical contamination. Rebalancing can be achieved either by mixing anolyte and catholyte²¹ or an added electrolysis cell.²²

Charge and discharge cycles for cell **2**/**2** are shown in Fig 3c. All three systems look similar, with the charge transferred increasing from **2** to **4**. This is expected, as the concentrations of **2-4** were kept constant at 1 mM, therefore additional Fc groups in molecules with higher degrees of functionalisation lead to increased capacity, shown in Figure 3d. Interestingly, the capacity decay for samples **3** and **4** seems to be faster than for **2**, as shown in Fig 3e which gives the discharge capacity normalised to the charge of the first discharge cycle. There are three explanations for the capacity loss. First, the electrolyte soaks into the dry separator, leading to a loss in active species within the electrode. Second, permeation of anolyte into the catholyte half-cell and vice-versa. Third, decomposition of the redox molecules. Importantly, the shape of all curves do not change over 100 cycles, and HPLC and mass spectrometry of the solutions after 100 cycles confirm that the molecules remain intact, however, an additional, unknown species is also observed to be formed which requires further investigations, see ESI file for full details. Most likely, all three mechanisms play a role. We hypothesize that soaking of the separator leads to the initial capacity loss in

the first few cycles, as the fade is similar for all three cells (Fig. 3e). Subsequent loss could be due to cross-over and decomposition. As cross-over is less of an issue for the 2/2 cell, its higher capacity retention than 3/ICBA and 4/ICBA can be rationalised.

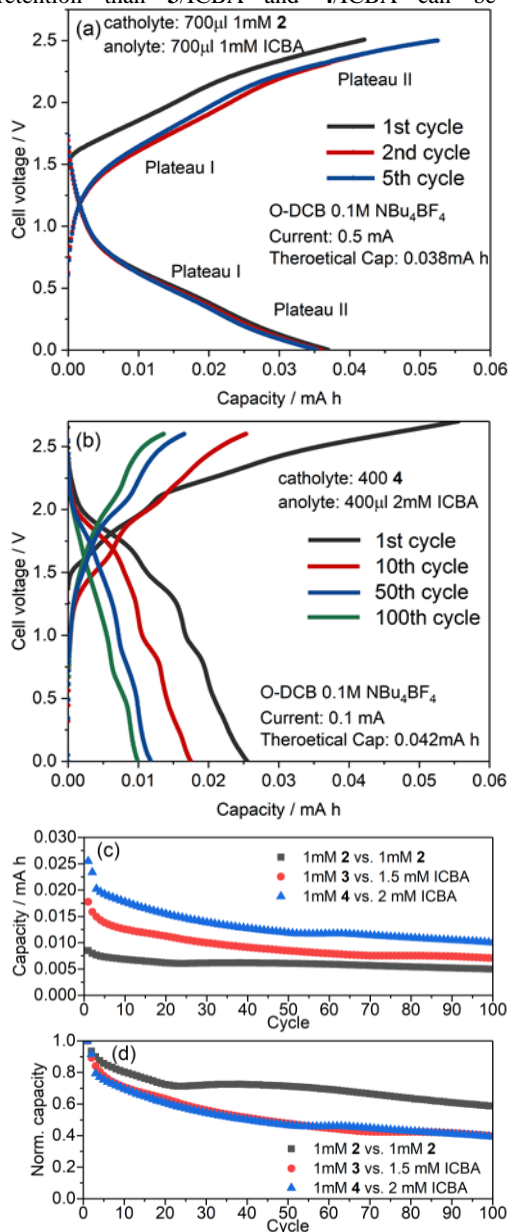


Figure 3. Charge and discharge curves for (a) the 2/ICBA, (b) the 4/ICBA in O-DCB with 0.1 M NBu₄BF₄. Capacity retention plots as (c) discharge capacity versus cycle number and (d) normalised capacity for the investigated systems.

While the three-electrode measurements and also the charge-discharge behaviour look promising, the low voltage efficiency shown in Fig. 3 is a problem. The cell voltage U depends on the current I :

$$U(I) = \Delta U \pm I \cdot R_{CT} \pm I \cdot R_{Diff} \pm I \cdot R_{Ohm} \quad (1)$$

With potential difference between the two half-cells, ΔU , charge transfer resistance for all redox processes, R_{CT} , mass transport resistance, R_{diff} , and the sum of all ohmic losses, R_{ohm} . The plus sign is applicable for the charging process, the minus sign for the discharge. Because R_{CT} is inversely proportional to k_0 and therefore small, and R_{Diff} is small because in our stationary cell all electrolyte is within the porous electrode, the overvoltage must stem from R_{Ohm} . R_{Ohm} comprises the resistance of the electrolyte and of the separator. This can be understood because in this configuration the

bulky tetrabutylammonium cation is required to cross the separator to balance the charge. Electrochemical impedance spectroscopy (EIS) measurements showed a significantly lower R_{Ohm} for DMF with 0.1 M LiCl (7 Ω) in the stationary cell than for O-DCB with 0.1 M NBu₄BF₄ (211 Ω) or 1.0 M NBu₄BF₄ (42 Ω) as shown in Fig. S14. Thus, cells with DMF as solvent and 0.1 M LiCl as electrolyte were tested. To avoid the contribution of water and oxygen, the cell assembly process and the preparation of the electrolytes were performed in a glove-box and an airtight cell was used.

Electrochemical impedance spectroscopy (EIS) measurements showed a significantly lower ohmic drop for DMF with 0.1 M LiCl (7 Ω) in the stationary cell than for O-DCB with 0.1 M NBu₄BF₄ (211 Ω) or 1.0 M NBu₄BF₄ (42 Ω) as shown in Fig. S14.

The 4/ICBA cell in DMF with 0.1 M LiCl was cycled 100 times at 1 mA revealing a current ten times higher than for a similar cell in O-DCB (Figure S12b). However, in DMF the shape of the charge-discharge curves do not remain stable. As can be seen in Figure S12a, the higher discharge plateau gradually vanishes, the lower plateau is then providing the capacity. These findings are supported by post-mortem HPLC and mass spectroscopy studies that found ICBA, but only traces of 4 after 100 cycles. The exact decomposition mechanism of 4 is unclear and requires further investigation. It is unlikely to be due to the retro-Prato reaction²³ as we do not observe formation of lower Fc adducts or unfunctionalised fullerene. Interestingly the capacity of cell 4/ICBA remains relatively stable throughout (Fig. S12b).

The cell chemistry shown in Figure S12 is able to produce a discharge current of 10 mA at a concentration of 1 mM. The electrode material was a GFD felt with surface area 1 cm² and thickness 4.6 mm. This shows that fullerene based chemistry could enable high power RFBs. Current VRB exhibit a current density of 0.07 A cm⁻².²⁴ Using the measured concentration of 4 (0.12 M), and assuming that the current scales with concentration, a current density of 1.2 A cm⁻² could be drawn from such a cell. Fig. S13 shows the rate capability of the 4/ICBA. A comparison of how this and other metrics relate to other reported RFB chemistries is shown in Table 1.

Being composed entirely of abundant, sustainable elements, our electrolyte system should face minimal resistance to scale-up, and thus we estimate bulk chemical costs of \$15 and \$11 kW h⁻¹ for the 4/ICBA and 2/2 electrolytes respectively based on raw materials.³ These costs can be compared directly with reported values of \$7-21 kW h⁻¹ for bromine and AQDS systems and \$83 kW h⁻¹ for vanadium flow batteries (see ESI for information on cost calculations).³ However, clearly such approximations do not give the full picture and costs such as the supporting electrolyte, which are currently unworkably high (cf. NBu₄BF₄ costs ~ \$12500 kW h⁻¹) need to be reduced, either by using cheaper salts or conductive solvents such as ionic liquid, for non-aqueous RFB systems to be competitive.²⁵ In summary, we have made a series of highly soluble redox active fullerene-ferrocene derivatives and fully characterised their electrochemical behaviour revealing multiple fast and reversible redox processes. We have explored their potential as multiple charge shuttles for redox flow batteries in two electrolytes. In O-DCB with 0.1 M NBu₄BF₄ we have observed high solubility (exceptionally high for fullerene derivatives), increasing capacity with increasing number of ferrocene adducts and charge discharge curves that do not alter their shape over 100 cycles. However, the conductivity of the solvent and supporting electrolyte was low, limiting the charging current to 0.1 mA. We have also demonstrated a symmetric cell, utilising 2 as anolyte and catholyte. As cross-over is less detrimental in a symmetric cell than in an asymmetric cell, this configuration can potentially enable a membrane-free design.²⁶ A membrane-free design eliminates the ohmic loss of the membrane, and therefore higher current densities than with a separator could be achieved.

Table 1. Performance metrics of the presented chemistries and literature studies.

Cell ^a	Solvent / electrolyte	OCV (V)	Current density per conc. (mA cm ⁻² mol ⁻¹)	Energy density per conc. (W h mol ⁻¹ L)
4/ICBA	<i>O</i> -DCB / 0.1 M NBu ₄ BF ₄	1.49	500	80
2/2	<i>O</i> -DCB / 0.1 M NBu ₄ BF ₄	1.64	500	44
4/ICBA	DMF / 0.1 M LiCl	1.49	10,000	80
VRB ²	Water / 2 M H ₂ SO ₄	1.26	44	17
AQDS/ Br ³	Water / 1 M H ₂ SO ₄	0.81	500	22
TEMPO/ VIOL ⁶	Water / 1 M NaCl	1.1	267	15
NMP/ benzene deriv. ⁹	DME / 1 M LiTFSI	2.3	167	31

^aSee the ESI for an explanation of the values and the performed calculations.

In DMF with 0.1 M LiCl, the stability of the Fc-modified fullerenes seems to be limited. During 100 charge and discharge cycles, the shape of the curves changed significantly. Also, post-mortem analysis could detect mostly the ICBA, but only traces of Fc-functionalised fullerene. On the other hand, high current rates up to 10 mA gave reasonable efficiencies. We can exclude that the Fc-functionalised fullerenes simply decompose and the Fc is active in solution, as cells with 4 mM Fc in DMF and 0.1 M LiCl showed a negligible discharge capacity (Fig. S10).

The current system demonstrates a novel concept in terms of redox electrochemistry for RFBs. Two electrolyte systems were investigated both exhibiting some limitations; stability in DMF and rate performance in *O*-DCB. However, intrinsically both the Fc/Fc⁺ and the C₆₀ redox reactions are facile, the molecules consist only of the cheapest, most abundant elements, i.e. C, N, Fe, and functionalisation methods have been developed to enhance fullerene solubility. Therefore, with further work, fullerene-based cells have the potential to revolutionise RFBs by simultaneously increasing the current and energy densities whilst enabling affordable and sustainable scale up.

ASSOCIATED CONTENT

Supporting Information

The Supporting Information (PDF) containing details of; fullerene synthesis and characterization, solubility, degradation and electrochemistry studies, and RFB performance and costing calculations, is available free of charge on the ACS Publications website at DOI:xxxxxxx.

AUTHOR INFORMATION

Corresponding Authors

ulrich.stimming@ncl.ac.uk and t.w.chamberlain@leeds.ac.uk.

Notes

The authors declare no competing financial interests.

ACKNOWLEDGMENT

We acknowledge the University of Leeds, Newcastle University and the EPSRC (EP/K030108/1) for support.

REFERENCES

- (1) Arenas-Martínez, L. F.; Ponce de León Albarran, C.; Walsh, F. C. *Journal of Energy Storage* **2017**, *11*, 119–153.
- (2) Weber, A. Z.; Mench, M. M.; Meyers, J. P.; Ross, P. N.; Gostick, J. T.; Liu, Q. *J. Appl. Electrochem.* **2011**, *41*, 1137–1164.
- (3) Huskinson, B.; Marshak, M. P.; Suh, C.; Er, S.; Gerhardt, M. R.; Galvin, C. J.; Chen, X.; Aspuru-Guzik, A.; Gordon, R. G.; Aziz, M. J. *Nature* **2014**, *505*, 195–8.
- (4) Lin, K.; Chen, Q.; Gerhardt, M. R.; Tong, L.; Kim, S. B.; Eisenach, L.; Valle, A. W.; Hardee, D.; Gordon, R. G.; Aziz, M. J.; Marshak, M. P. *Science* **2015**, *349*, 1529–1532.
- (5) Beh, E. S.; De Porcellinis, D.; Gracia, R. L.; Xia, K. T.; Gordon, R. G.; Aziz, M. J. *ACS Energy Lett.* **2017**, 639–644.
- (6) Janoschka, T.; Martin, N.; Martin, U.; Friebe, C.; Morgenstern, S.; Hiller, H.; Hager, M. D.; Schubert, U. S. *Nature* **2015**, *527*, 78–81.
- (7) Milshtein, J. D.; Kaur, A. P.; Casselman, M. D.; Kowalski, J. A.; Modetrutti, S.; Zhang, P. L.; Harsha Attanayake, N.; Elliott, C. F.; Parkin, S. R.; Risko, C.; Brushett, F. R.; Odom, S. A. *Energy Environ. Sci.* **2016**, *9*, 3531–3543.
- (8) Duan, W.; Huang, J.; Kowalski, J. A.; Shkrob, I. A.; Vijayakumar, M.; Walter, E.; Pan, B.; Yang, Z.; Milshtein, J. D.; Li, B. *ACS Energy Lett.* **2017**, *2*, 1156–1161.
- (9) Wei, X.; Duan, W.; Huang, J.; Zhang, L.; Li, B.; Reed, D.; Xu, W.; Sprengle, V.; Wang, W. *ACS Energy Lett.* **2016**, *1*, 705–711.
- (10) Wei, X.; Xu, W.; Huang, J.; Zhang, L.; Walter, E.; Lawrence, C.; Vijayakumar, M.; Henderson, W. A.; Liu, T.; Cosimbescu, L.; Li, B.; Sprengle, V.; Wang, W. *Angew. Chemie - Int. Ed.* **2015**, *54*, 8684–8687.
- (11) Winsberg, J.; Hagemann, T.; Janoschka, T.; Hager, M. D.; Schubert, U. S. *Angew. Chemie - Int. Ed.* **2017**, *56*, 686–711.
- (12) Leung, P.; Shah, A. A.; Sanz, L.; Flox, C.; Morante, J. R.; Xu, Q.; Mohamed, M. R.; Ponce de León, C.; Walsh, F. C. *J. Power Sources*, **2017**, *360*, 243–283.
- (13) Noack, J.; Roznyatovskaya, N.; Herr, T.; Fischer, P. *Angew. Chemie - Int. Ed.*, **2015**, *54*, 9776–9809.
- (14) Echegoyen, L.; Echegoyen, L. E. *Acc. Chem. Res.* **1998**, *31*, 593–601.
- (15) Ganesamoorthy, R.; Sathiyam, G.; Sakthivel, P. *Sol. Energy Mater. Sol. Cells* **2017**, *161*, 102–148.
- (16) Yamakoshi, Y.; Aroua, S.; Nguyen, T.-M. D.; Iwamoto, Y.; Ohnishi, T. *Faraday Discuss.* **2014**, *173*, 287–296.
- (17) Birkin, P. R.; Silva-Martinez, S. *Anal. Chem.* **1997**, *69*, 2055–62.
- (18) Friedl, J.; Stimming, U. *Electrochim. Acta* **2017**, *227*, 235–245.
- (19) Carano, M.; Da Ros, T.; Fanti, M.; Kordatos, K.; Marcaccio, M.; Paolucci, F.; Prato, M.; Roffia, S.; Zerbetto, F. *J. Am. Chem. Soc.* **2003**, *125* (23), 7139–7144.
- (20) Huang, Q.; Li, H.; Grätzel, M.; Wang, Q. *Phys. Chem. Chem. Phys.* **2013**, *15*, 1793–7.
- (21) Tang, A.; Bao, J.; Skyllas-Kazacos, M. *J. Power Sources*, **2011**, *196*, 10737–10747.
- (22) Rudolph, S.; Schröder, U.; Bayanov, I. M. *J. Electroanal. Chem.*, **2013**, *703*, 29–37.
- (23) Martín, N.; Altable, M.; Filippone, S.; Martín-Domenech, A.; Echegoyen, L.; Cardona, C. M. *Angew. Chem. Int. Ed.*, **2006**, *45*, 110–114.
- (24) Zhao, P.; Zhang, H.; Zhou, H.; Chen, J.; Gao, S.; Yi, B. *J. Power Sources* **2006**, *162*, 1416–1420.
- (25) Dmello, R.; Milshtein, J. D.; Brushett, F. R.; Smith, K. C. *J. Power Sources* **2016**, *330*, 261–272.
- (26) Navalpotro, P.; Palma, J.; Anderson, M.; Marcilla, R. *Angew. Chemie - Int. Ed.*, **2017**, *56*, 12460–12465.

